Motivation For Lowering Milagro's Trigger Threshold

Elizabeth Hays David Noyes

September 9, 2000

1 Introduction

Milagro's all-sky capability gives it a unique opportunity to observe transient events. To observe a reasonable number and variety of transient events Milagro needs to view as much of the universe as possible. The primary physics limitation of Milagro's viewing depth is attenuation of high energy photons by the Extragalactic Background Light (EBL). Many papers discuss this process in detail, but the upshot is that high energy photons scatter off of infrared photons from stars imposing a high energy cutoff in extragalactic spectra. Beyond this cutoff distance an extragalactic source becomes invisible within some energy range, typically around a few TeV. Therefore, the further away the source is, the more important it is to see the lower energy photons. The EBL is not well-measured, but by using theoretical models we can get some idea of the energy and redshift dependence of attenuation. We can then look at how this attenuation affects Milagro gamma ray event rates. The following is intended to provide a rough idea of how Milagro's observation of distant sources improves as the trigger threshold is lowered and to motivate progress toward that goal.

2 Calculating Milagro's Rate

2.1 Effective Area

To determine Milagro's event rate for gammas, we first need to calculate the effective area. For this we looked at gamma ray monte carlo events created using GEANT version 2.4 and Corsika version 5.61100. The events were thrown on an $E^{-2.4}$ spectrum with a throw area of $10^6\ m^2$. Two separate Monte Carlo data sets were used, one with energy range from 10 GeV to 100 GeV, and another from 100 GeV to 100 TeV. We looked at 26 million events from the low energy data, and 8 million events from the high energy data (in the future we would like to include more low energy events in our analysis, since there are so few triggers in this energy range). To obtain the effective area the number of triggers for Nhit in the airshower layer greater than the tube threshold are counted, and divided by the total number of events thrown. This is then multiplied by the throw area to give the effective area. This was done for thresholds between 10 and 60 tubes, and zenith angle cuts of 0-15, 15-30, and 30-45 degrees.

In figure 1 the number of gamma events above threshold is plotted as a function of energy. With a threshold of 60 tubes, no triggers are recorded below about 200 GeV, but at a lower threshold we do record events all the way down to 10 GeV. So, by lowering the threshold, it is clear that we are able to see more low energy events.

Figure 2 shows the effective area for thresholds of 30 and 60 tubes at each of the zenith angle cuts, and for the sum of the three angle bins. Here we see that at a higher threshold the effective area goes to zero around 100 GeV, while for a lower threshold the effective area extends to lower energy.

In figure 3 the effective area is integrated over energy and plotted as a function of threshold, showing the increase in effective area as the threshold is lowered.

2.2 Attenuation Due to IR Background

The process $\gamma + \gamma \rightarrow e^{+} + e^{-}$ leads to absorption of extragalactic TeV photons by scattering with infrared photons. Although the density of the infrared background has only been measured to upper and lower limits, theoretical models exist dependent on the cosmology and initial mass function (IMF). Here we have used a model from a thesis by James Bullock (a student of J. Primack) based on a ΛCDM universe with Salpeter IMF. Bullock has calculated the opacity as a function of photon energy and redshift. Using this opacity the survival probability is $e^{-\tau(E,z)}$. Figure 4 shows the survival probability as a function of energy for z = 0.03, 0.1, 0.2, 0.5, and 1.0.

2.3 Event Rate

To obtain an event rate as a function of z and trigger threshold, we need to compute the following integral:

$$rate = \int_{10GeV}^{100TeV} \mathrm{dE} \;\; \mathrm{A}_{eff}(\mathrm{N}_{trigger}) \times \frac{dN}{dEdAdt} \times e^{-\tau(E,z)}$$

For $\frac{dN}{dEdAdt}$ we use the Crab spectrum of 3.3e-7 $E^{-2.4}$ events/TeV/m^2/sec. For a different source with the same spectrum, the rate can be multiplied by the number of crab units of that source. This spectrum is convolved with the effective area for each trigger threshold. The resulting histograms are then convolved with the survival probability at z = 0.03, 0.1, 0.2, 0.5, and 1.0. This gives the number of events/GeV/sec as a function of energy, which can then be integrated to give the total event rate for a given z and trigger threshold.

3 Results

The differential event rate (figure 5) is integrated over energy to obtain figure 6, which shows the total event rate as a function threshold for different values of z. The plot shows that lowering the threshold allows detection of sources at higher z. Note that for small z distance is approximately linear in z, so a factor farther in z means a factor cubed in volume. For a uniform distribution of sources this also means a factor cubed more observable sources.

From our calculations we can show how the event rate for a particular threshold changes with z (see Figure 7). As the distance to the source increases, the event rate drops more drastically for higher thresholds. While the event rate for a 10 tube threshold drops by more than an order of magnitude, the rate for a 60 tube threshold drops by about 3 orders of magnitude. The benefit in lowering the trigger threshold is evident in these figures and the table below. For example, the event rate for a 60 tube threshold at z=0 is almost the same as that for a 30 tube threshold at z=0.03 or for a 10 tube threshold at z=0.2. Milagro's sensitivity for these low energy events remains to be studied, but this preliminary result indicates that to see further the trigger must be lowered as much as possible.

Table 1: This shows the number of events (rounded to the nearest event) assuming a GRB with a flux 100 times the crab and duration of 100 seconds.

Trigger Threshold	10	20	30	40	50	60	70
z=0	50	22	15	11	8	7	6
z=0.03	32	13	8	6	4	3	3
z=0.1	17	6	4	2	2	1	1
z=0.2	10	3	2	1	0	0	0
z=0.5	3	2	1	0	0	0	0

4 More Results

While working on this memo we spent a great deal of time studying for and being stressed about qualifiers. Thank you to those of you who offered advice and encouragement (especially Rob who had the most advice to offer and also let us copy his solutions manuals and study sheets.) Apparently it was not in vain because we both passed and are now free to "forget all that nonsense and do some real physics."

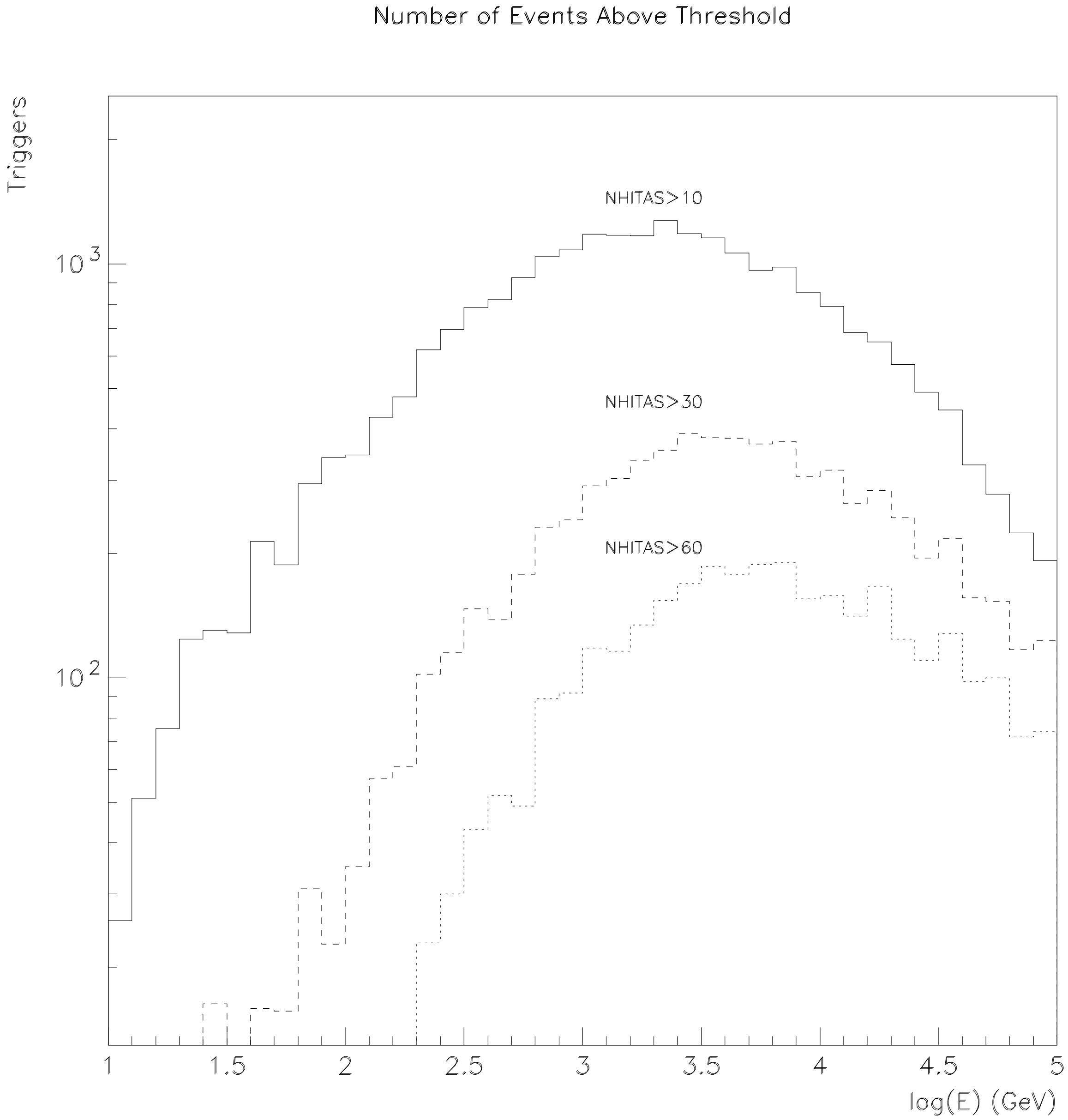

Figure 1: When the trigger threshold is lowered, the increase in gamma triggers is most pronounced at lower energies.

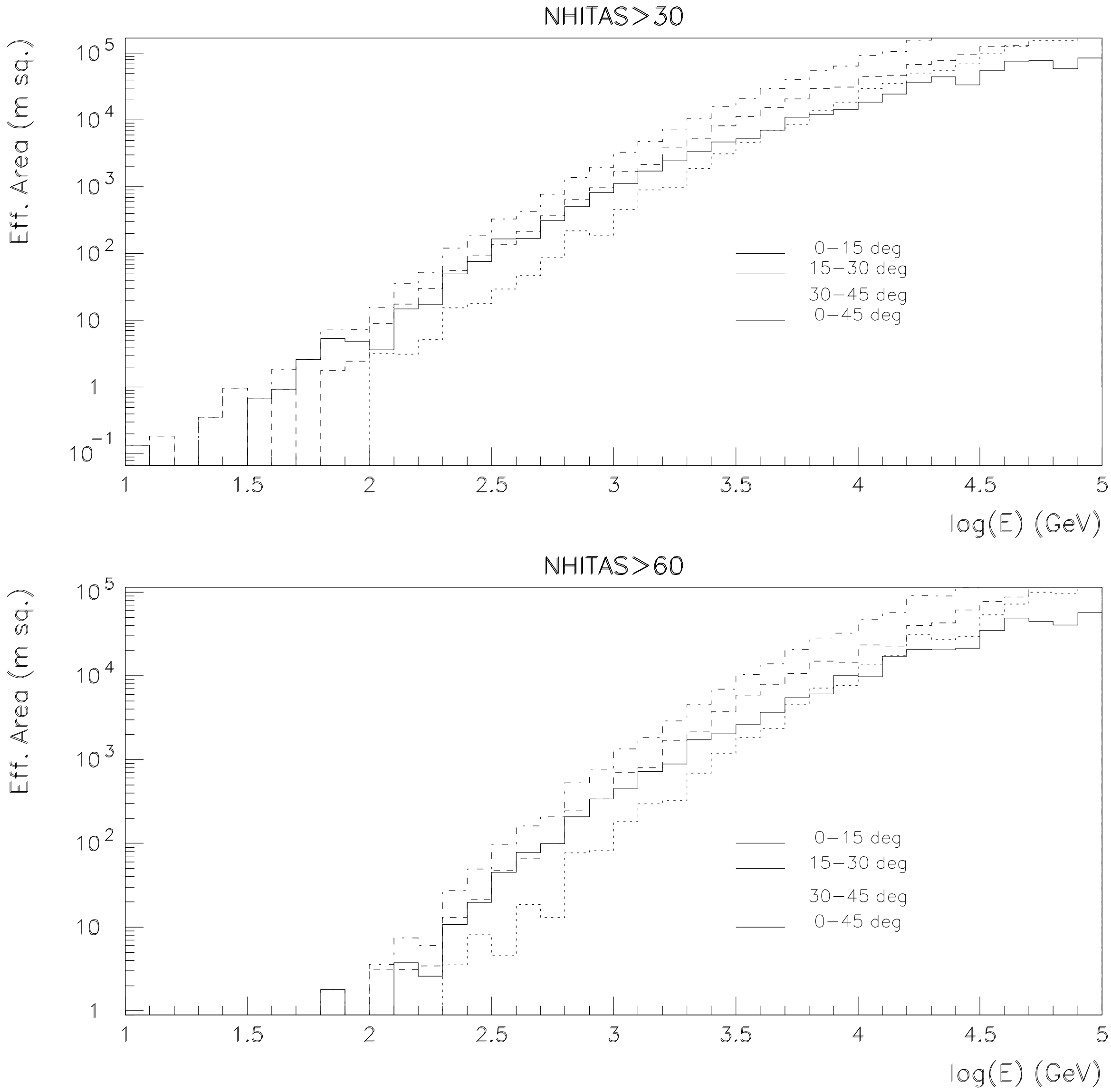

Figure 2: This shows the dependence of the effective area on zenith angle cut. Only events within 0-15 deg. of zenith were considered for our calculations.

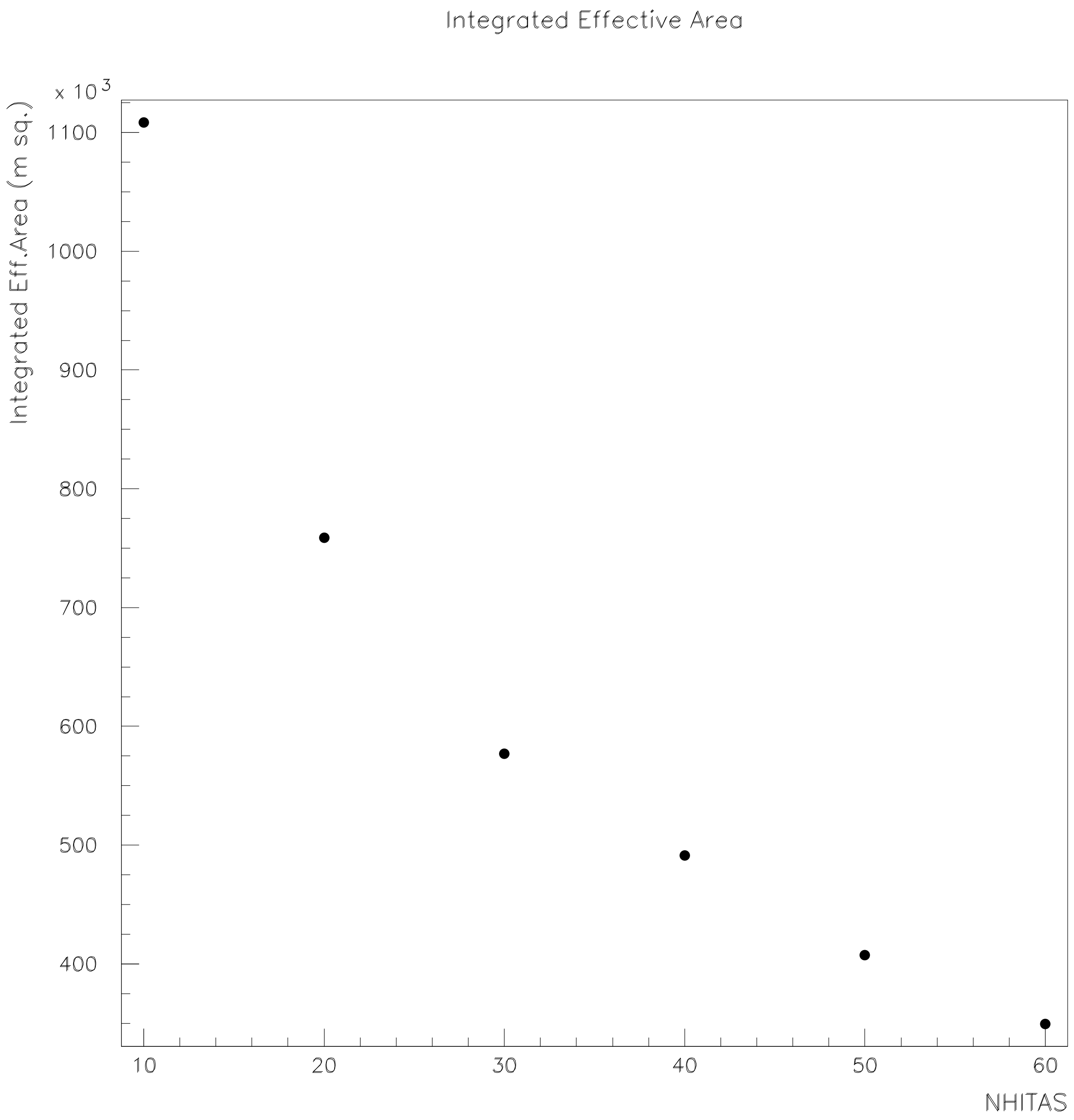

Figure 3: Effective area is calculated at 6 trigger thresholds from 10 to 60 tubes. Lowering the threshold to 10 tubes increases effective area by a factor of three.

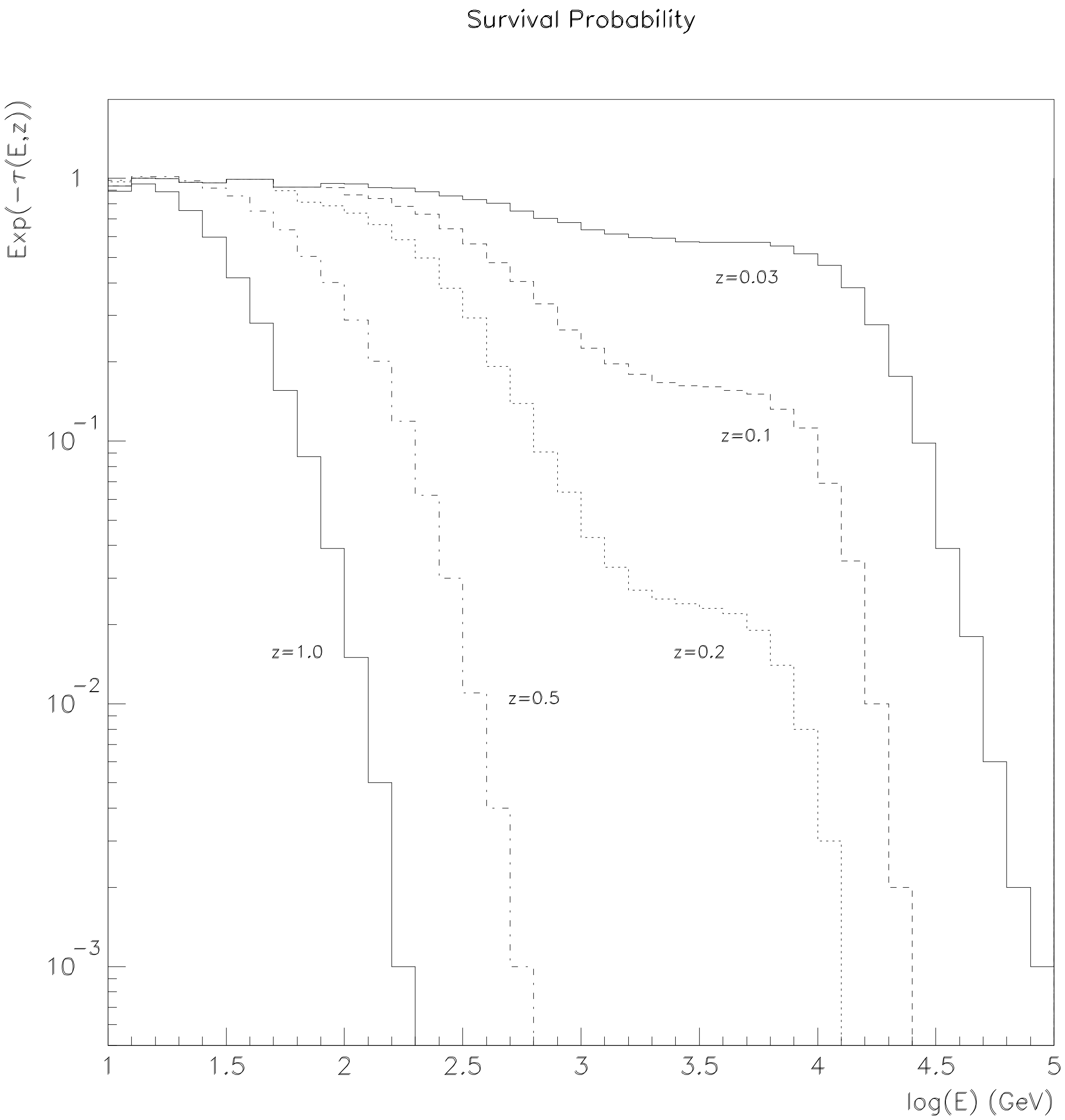

Figure 4: The survival probability as a function of redshift and photon energy is taken from James Bullock's thesis (UCSC, June 1999.)

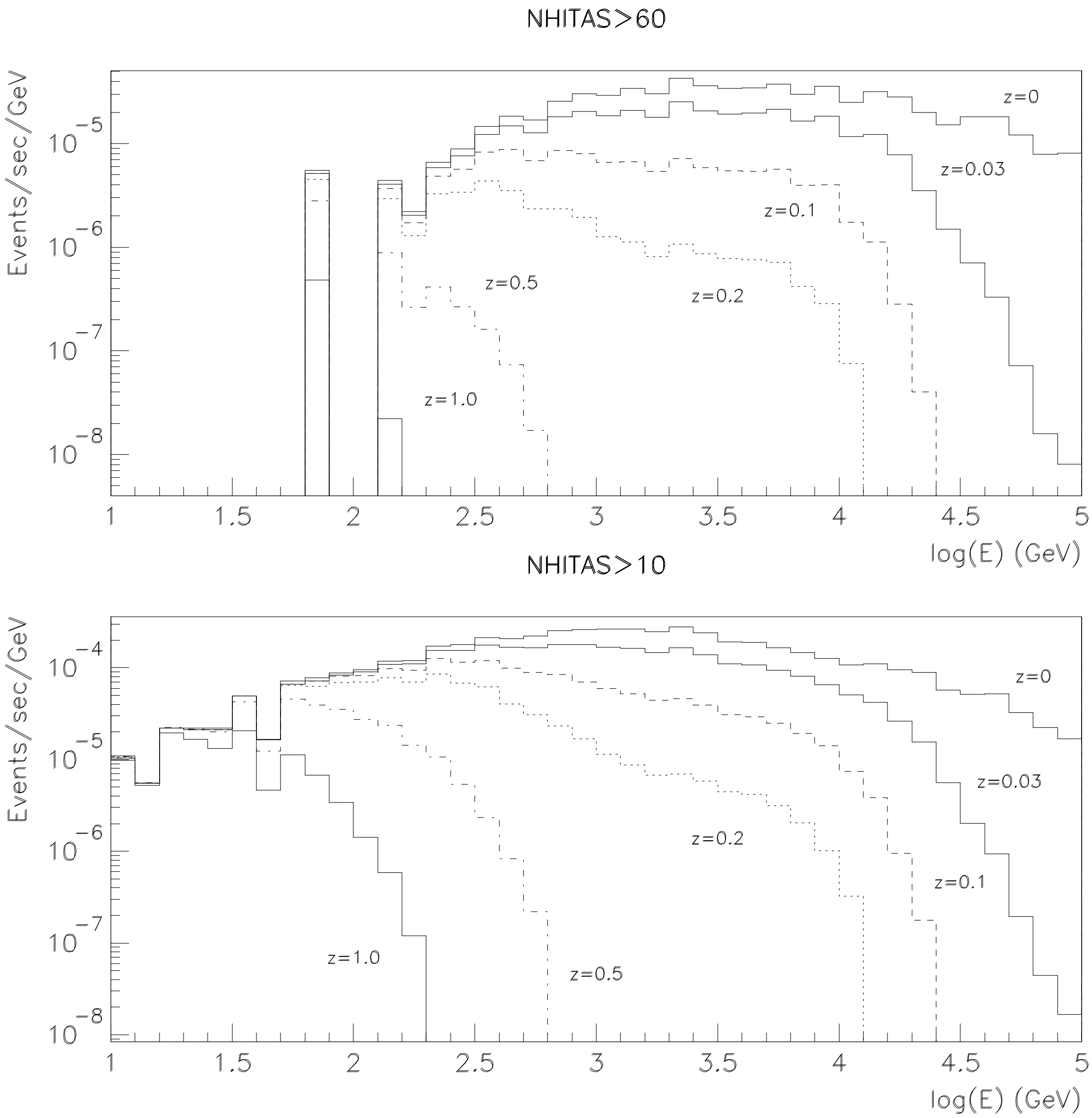

Figure 5: The difference between differential rates for a 60 trigger threshold and a 10 trigger threshold shows the advantage of a lower trigger at the low end of our energy range. Redshift z=0 represents the combined effective area and source spectrum without attenuation.

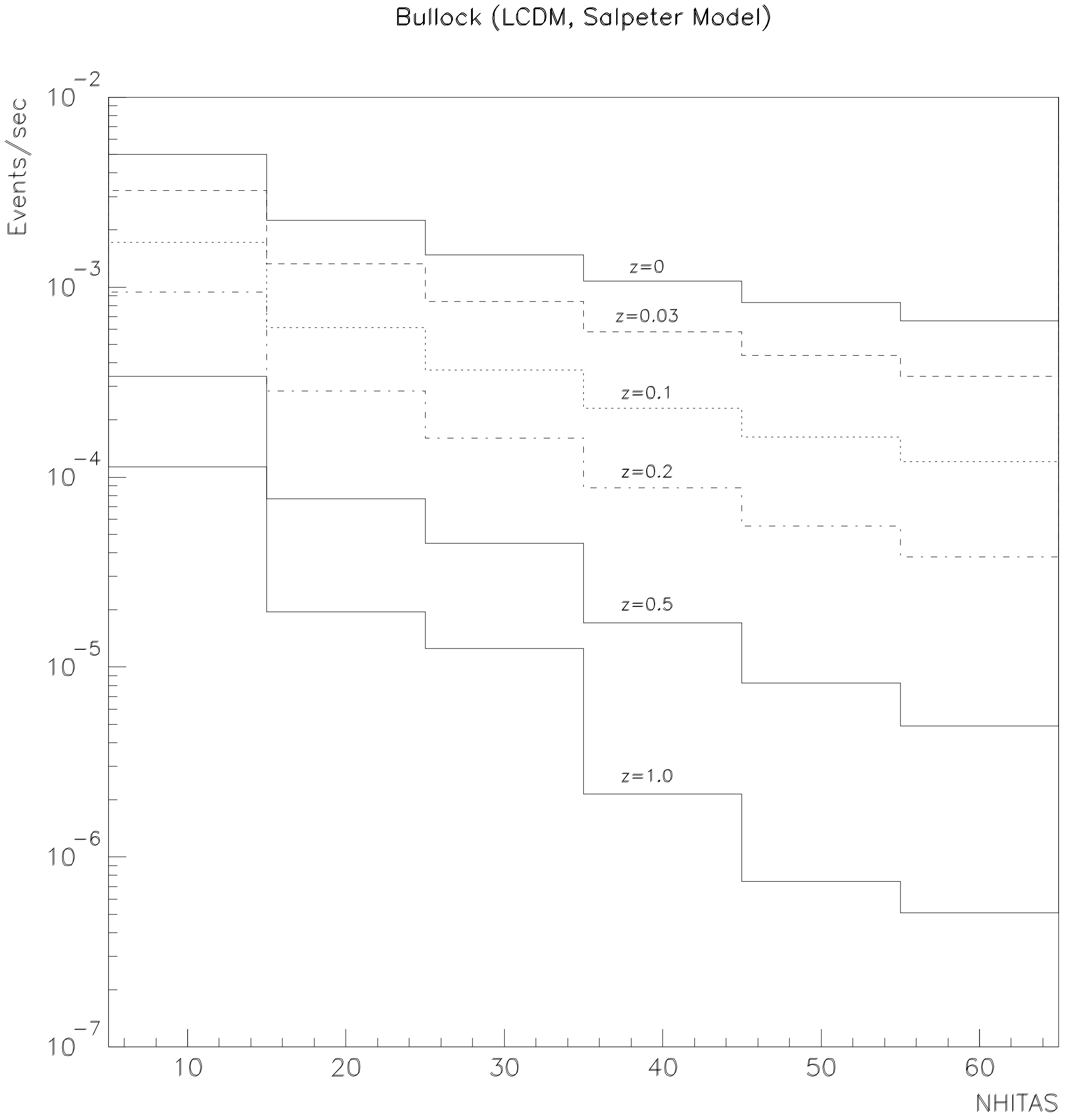

Figure 6: The gamma ray event rates for each z are shown at each threshold. Note that the rate increase for lowered trigger threshold is more dramatic at larger redshifts. Calculations were made for a 70 tube threshold as well but are not shown here as they are very similar to the 60 tube threshold.

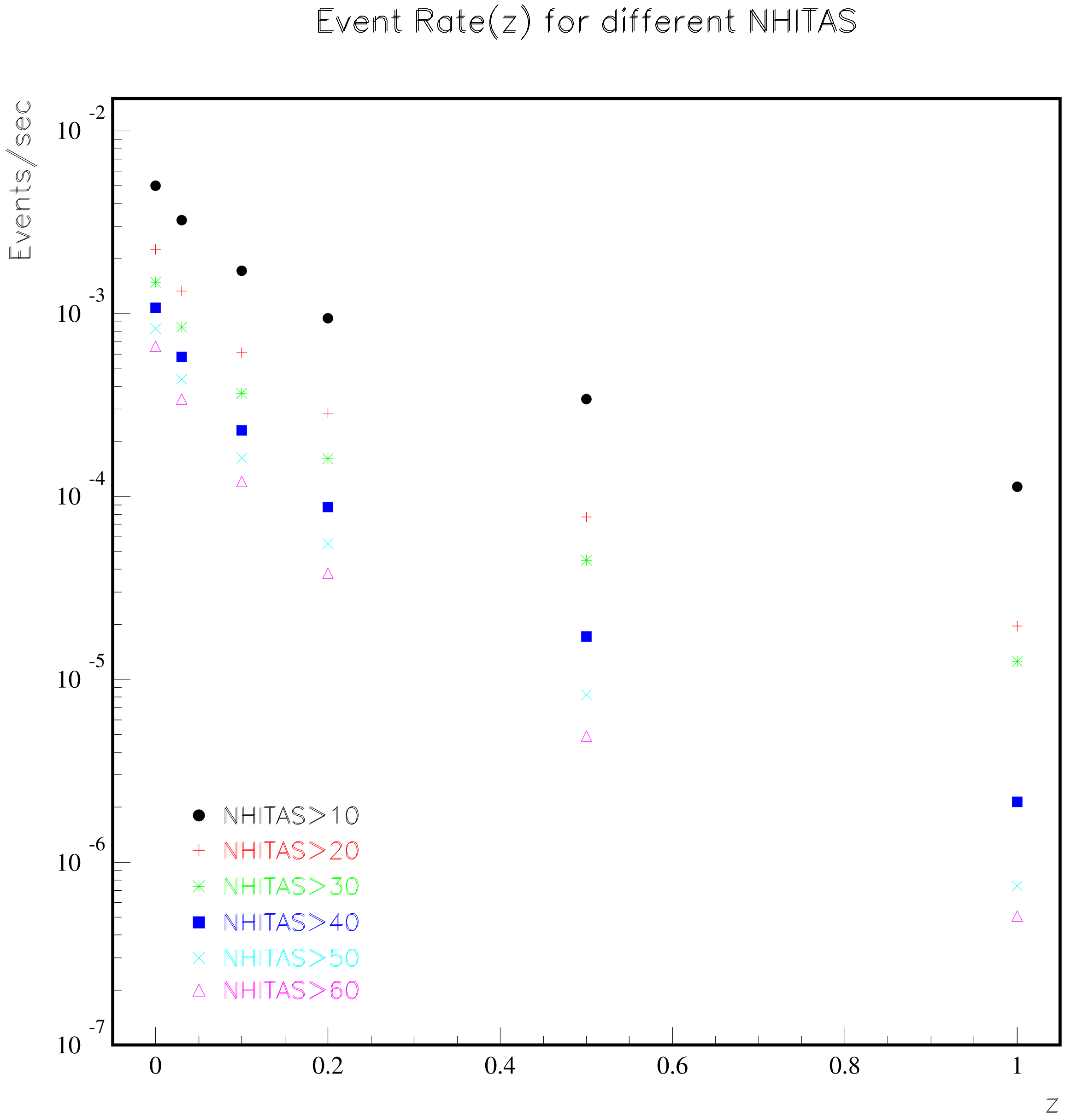

Figure 7: The gamma ray event rate for each trigger threshold is shown as a function of redshift.